EXPERIMENTAL ANALYSIS OF COLLECTIVE CIRCULAR MOTION FOR MULTI-VEHICLE SYSTEMS

N. Ceccarelli, M. Di Marco, A. Garulli, A. Giannitrapani

DII - Dipartimento di Ingegneria dell'Informazione
Università di Siena
Via Roma 56, Siena, Italy

Abstract: This paper presents an experimental analysis of a recently proposed decentralized control strategy, for collective circular motion of a team of nonholonomic vehicles. Theoretical results ensuring global asymptotic stability in the single-vehicle case and local asymptotic stability in the multi-vehicle scenario, are validated on an experimental setup including the mobile robots Pioneer 3AT and Nomad XR4000. In addition, the role of the control law parameters is discussed and a design procedure is proposed.

Keywords: Multi-vehicle systems, nonholonomic vehicles, collective motion.

1. INTRODUCTION

Multi-robot systems have received increasing interest in recent years due to their impact in many different fields, including exploration, distributed sensing, coordinated manipulation, etc. (see e.g. (Arai *et al.*, 2002) and references therein). Several theoretical frameworks have been proposed to analyze the collective motion of multi-agent systems, considering linear motion models (Leonard and Fiorelli, 2001; Jadbabaie *et al.*, 2003; Lin *et al.*, 2004) or unicycle-like motion models (Justh and Krishnaprasad, 2004; Marshall *et al.*, 2004). Although nice theoretical results have been obtained, still few experimental validations are present in the literature (Marshall *et al.*, 2005).

In this paper, we present an experimental analysis of a decentralized control law for a team of nonholonomic vehicles, introduced by Ceccarelli *et al.* (2005*a*). This control strategy guarantees asymptotic stability of the collective circular motion around a virtual reference beacon. The purpose of this work is to verify the viability of the proposed technique in a real-world scenario and its effectiveness in dealing with important practical issues such as unmodeled dynamics, measurement errors, etc. In this respect, the considered control law seems particularly appealing since it is easy to implement and does not require information exchange among the vehicles. As an additional contribution, the paper presents a discussion about the role of the control law parameters and proposes some design guidelines.

The paper is organized as follows. Section 2 reviews the considered control law and its properties. In Section 3 the role of the control parameters is analyzed. Experimental results are presented in Section 4 and some conclusions are drawn in Section 5.

2. DECENTRALIZED CONTROL LAW

In order to illustrate the main features of the decentralized control scheme proposed by Ceccarelli *et al.* (2005*a*), the single-vehicle case and the multi-vehicle scenario are considered separately. The interested reader is referred to (Ceccarelli *et al.*, 2005*b*) for the technical details.

2.1 Single vehicle scenario

Let us consider a nonholonomic vehicle featuring unicycle-like kinematics

$$\dot{x}(t) = v\,\cos\theta(t) \tag{1}$$
$$\dot{y}(t) = v\,\sin\theta(t) \tag{2}$$
$$\dot{\theta}(t) = u(t) \tag{3}$$

where $[x\ \ y\ \ \theta] \in \mathbb{R}^2 \times [-\pi, \pi)$ represents the vehicle pose, v is the forward speed (assumed to be constant) and $u(t)$ is the angular speed, which plays the role of control input. The objective is to achieve a rotational motion around a virtual reference beacon. The following control law, based on the relative pose of the vehicle with respect to the beacon, is adopted:

$$u(t) = \begin{cases} k_b \cdot g(\rho(t), c_b, \rho_0) \cdot \alpha_{dist}(\gamma(t), \psi) & \text{if } \rho > 0 \\ 0 & \text{if } \rho = 0 \end{cases} \tag{4}$$

with

$$g(\rho(t), c_b, \rho_0) = \ln\Big(\frac{(c_b - 1)\cdot\rho(t) + \rho_0}{c_b \cdot \rho_0}\Big) \tag{5}$$

and

$$\alpha_{dist}(\gamma(t), \psi) = \begin{cases} \gamma(t) & \text{if } 0 \le \gamma(t) \le \psi \\ \gamma(t) - 2\pi & \text{if } \psi < \gamma(t) < 2\pi. \end{cases} \tag{6}$$

In (4)-(6), ρ is the distance of the vehicle to the beacon and $\gamma \in [0, 2\pi)$ represents the angular displacement between the heading of the vehicle and the direction of the beacon (see Fig. 1(a)). The parameters $k_b > 0$, $c_b > 1$, $\rho_0 > 0$ and $\psi \in (\frac{3}{2}\pi, 2\pi)$ are given constants. The following result holds.

Proposition 1. Let $\psi \in (\frac{3}{2}\pi, 2\pi)$. If the control parameters k_b, c_b, ρ_0 are chosen so that

$$\min_{\rho}\ \rho \cdot g(\rho, c_b, \rho_0)\ >\ -\frac{2\,v}{3\,\pi\,k_b}\,, \tag{7}$$

then the counterclockwise rotation about the beacon with rotational radius ρ_e, defined as the unique solution of

$$\rho_e \cdot g(\rho_e, c_b, \rho_0)\ =\ \frac{2\,v}{\pi\,k_b}\,, \tag{8}$$

and angular velocity $\frac{v}{\rho_e}$, is a globally asymptotically stable limit cycle for the system (1)-(6).

Notice that the choice $\psi \in (\frac{3}{2}\pi, 2\pi)$ together with inequality (7) ensures that the clockwise rotation about the beacon is not an equilibrium configuration.

2.2 Multi-vehicle scenario

Now let us consider the case of a team of n vehicles. Their motion is described by the equations

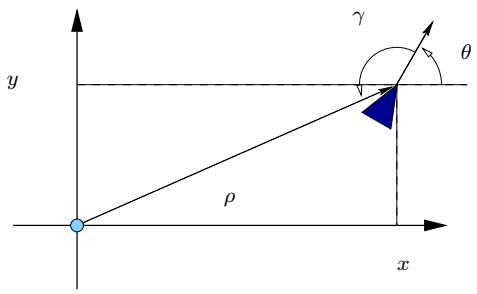

(a) One vehicle (triangle) and beacon (placed in the origin)

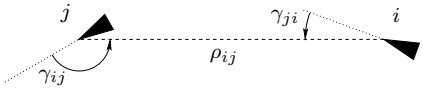

(b) Two vehicles (triangles)

Fig. 1. Relative distance and angular displacements.

$$\dot{x}_i(t) = v\,\cos\theta_i(t) \tag{9}$$
$$\dot{y}_i(t) = v\,\sin\theta_i(t) \tag{10}$$
$$\dot{\theta}_i(t) = u_i(t), \tag{11}$$

with $i = 1 \dots n$. Let ρ_{ij} and γ_{ij} denote respectively the linear and angular distance between vehicle i and vehicle j (see Fig. 1(b)). The team has to achieve collective circular motion around a fixed beacon. Further requirements to take into account are collision avoidance and sensory limitations. A visibility region $\mathcal{V}_i$ is associated to each vehicle, representing the portion of environment that each vehicle perceives through its sensing equipment. The visibility region is chosen as the union of two sets: i) a circular sector of radius d_l and angular amplitude $2\alpha_v$; ii) a circle of radius d_s around the vehicle (see Fig. 2).
The single-vehicle control law (4) is modified by adding a new term accounting for the interaction between vehicles. Let $\mathcal{N}_i$ denote the set containing the indexes of the vehicles lying inside $\mathcal{V}_i$. The control input of the i-th vehicle is

$$u_i(t) = f_{ib}(\rho_i, \gamma_i) + \sum_{j \in \mathcal{N}_i} f_{ij}(\rho_{ij}, \gamma_{ij}) \tag{12}$$

where f_{ib} is the same as in the right hand side of (4), while

$$f_{ij}(\rho_{ij}, \gamma_{ij}) = k_v \cdot g(\rho_{ij}, c_v, d_0) \cdot \alpha_{dist}(\gamma_{ij}, \pi). \tag{13}$$

The functions $g(\cdot)$ and $\alpha_{dist}(\cdot)$ have been defined in (5)-(6) while $k_v > 0$, $c_v > 1$, $d_0 > 0$ are given constants. The basic idea underlying the control law (12)-(13) is that each agent i is driven by the term $f_{ib}(\cdot)$ towards the counterclockwise circular motion around the beacon (according to Proposition 1), while the terms $f_{ij}(\cdot)$ favor collision free trajectories, trying to keep distance $\rho_{ij} = d_0$ for all the agents $j \in \mathcal{N}_i$. Intuitively, vehicle i

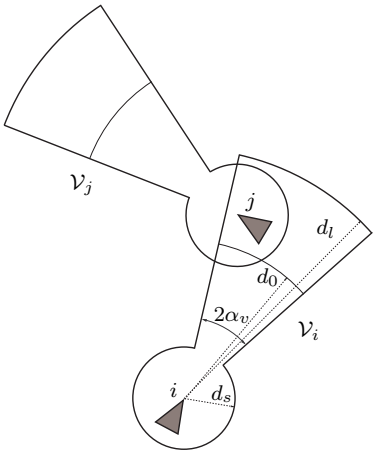

Fig. 2. Visibility region of i-th and j-th vehicle.

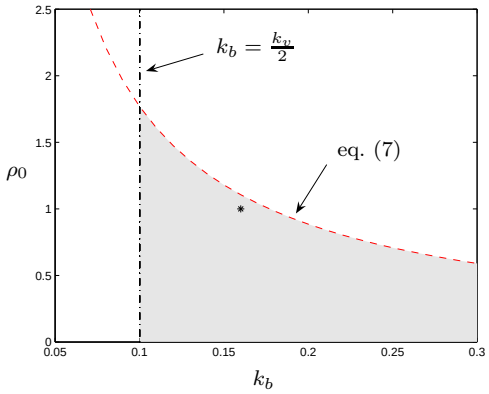

Fig. 3. Feasible region for parameters k_b and ρ_0.

is attracted by any vehicle $j \in \mathcal{N}_i$ if $\rho_{ij} > d_0$, and repulsed if $\rho_{ij} < d_0$. The expected result of such combined actions is that the agents reach the counterclockwise circular motion in a number of platoons, in which the distances between consecutive vehicles is d_0. Let us suppose that the parameters d_0, d_l and the number of vehicles n are such that

$$(n-1)\,\arcsin\left(\frac{d_0}{2\rho_e}\right) + \beta < \pi, \qquad (14)$$

with

$$\beta = \min\left\{\alpha_v, \arcsin\left(\frac{\min\{d_l, 2\rho_e\}}{2\rho_e}\right)\right\}.$$

This choice guarantees that n vehicles can lie on a circle of radius ρ_e, with distance d_0 between two consecutive vehicles and so that there is at least one vehicle wich does not perceive any other vehicle. The following result holds.

Proposition 2. Let d_0, d_l and n be such that condition (14) holds. Then, every configuration of n vehicles in counterclockwise circular motion around a fixed beacon, with rotational radius $\rho_i = \rho_e$ defined in (8), $\gamma_i = \frac{\pi}{2}$ and $\rho_{ij} = d_0$ $\forall i = 1 \dots n$ and $\forall j \in \mathcal{N}_i$, corresponds to a limit cycle for the system (9)-(13). Moreover. if the parameters k_b, c_b, k_v, c_v in the control law (12)-(13) are such that

$$\frac{k_v}{k_b} \leq 2\,\frac{c_v}{c_b}\,\frac{c_b - 1}{c_v - 1}, \qquad (15)$$

then the aforementioned limit cycles are locally asymptotically stable.

Notice that the proposed control law does not require exteroceptive orientation measurements, nor labeling of the vehicles. Each agent can easily compute its control input from range measurements, without any exchange of information.

3. SELECTION OF THE PARAMETERS

The control law under investigation is characterized by several parameters, which must be properly tuned in order to achieve a satisfactory collective behavior. In this section we discuss the role played by the control parameters and present a possible procedure for selecting their values.

First notice that the clockwise rotation around the beacon must not be an equilibrium point, i.e. the parameters have to verify inequality (7). This can be obtained by choosing a sufficiently small ρ_0 or, alternatively, a sufficiently small control gain k_b in (4). The equilibrium radius ρ_e must be consistent with the number of vehicles and the desired inter-vehicle distance d_0. This means that the configuration of a single platoon in circular motion must be feasible with respect to inequality (14). Notice that this requires a sufficiently large ρ_e (for fixed d_0), and therefore a sufficiently large ρ_0. This introduces a trade-off with the requirement imposed by (7). On the other hand, since ρ_e can be increased by suitably reducing k_b, it is always possible to find a sufficiently small k_b satisfying both (7) and (14). However, a too small k_b may lead to violation of the sufficient condition (15), and hence stability of the desired circular collective motion is not guaranteed anymore. Figure 3 shows the region of feasible parameters k_b and ρ_0, for the scenario considered in Section 4 ($c_b = c_v = 4$, $k_b = 0.2$). The region below the dashed curve contains the values of k_b and ρ_0 satisfying (7). In the case of two vehicles with $\alpha_v < \frac{\pi}{2}$, constraint (14) is satisfied for all pairs (k_b, ρ_0). Finally, the sufficient condition (15) of Theorem 2 is satisfied by all values of k_b lying on the right of the dash-dotted line (notice that for $c_b = c_v$, condition (15) boils down to $k_b \geq \frac{k_v}{2}$). Therefore, by choosing k_b and ρ_0 inside the dashed region it is possible to satisfy all the geometrical constraints and the stability condition.

4. EXPERIMENTAL RESULTS

The experimental setup features two robots available at the DII Mobile Robotics Lab: a Pioneer 3AT and a Nomad XR4000. The first one is a four-wheeled robot whose kinematics can be described by the unicycle model. The latter is an holonomic mobile robot which has been programmed in order to behave as a unicycle. A laser rangefinder is available on both robots, with angular visibility π, hence $\alpha_v = \frac{\pi}{2}$ in Fig. 2. The environment is an empty room, with a reference beacon placed in the middle (see Fig. 4). The extraction of the reference beacon as well as the measurements of the inter-vehicle linear and angular distances ρ_{ij}, γ_{ij} are obtained from the laser raw readings, via standard filtering techniques. Because of the limited field of view of the sensors, the robots cannot detect the beacon position from every pose. To overcome this problem, odometry-based estimation of the robot pose is performed whenever the beacon is not perceived. The control strategy described in Section 2 has been implemented locally on each robot, from data extraction to control input computation, without neither communication between the robots nor centralized supervisor (like a vision system or GPS). Considering the dimension of the available space in the room and the achievable angular and tangential velocities, we chose $v = 0.2\,m/s$ and, according to Fig. 3, $k_b = 0.16$, $\rho_0 = 1\,m$ (corresponding to the black asterisk). By equation (8), one has $\rho_e = 1.76\,m$.

Figure 5 reports an experimental test for the single-robot scenario featuring the Nomad. The ρ and γ measurements in Fig. 5(a) are performed by the laser rangefinder on the robot, while the actual trajectory in Fig. 5(b) is measured by another stationary laser rangefinder. One can see the correct asymptotic behavior of the measured ρ and γ, converging respectively to ρ_e and $\frac{\pi}{2}$ (dashed lines in Figs. 5 and 6). The trajectory confirms that the Nomad achieves the desired counterclockwise circular motion.

Figure 6 concerns a similar experimental test with the Pioneer. Figure 6(b) shows that also in this case the circular motion is achieved. Nonetheless, the errors $|\rho(t) - \rho_e|$ and $|\gamma(t) - \frac{\pi}{2}|$ do not vanish asymptotically, as shown in Fig. 6(a). This is due to the particular position of the laser sensor on the robot, which is aligned with the orientation of the Pioneer and placed almost in the center of

Fig. 4. The experimental environment.

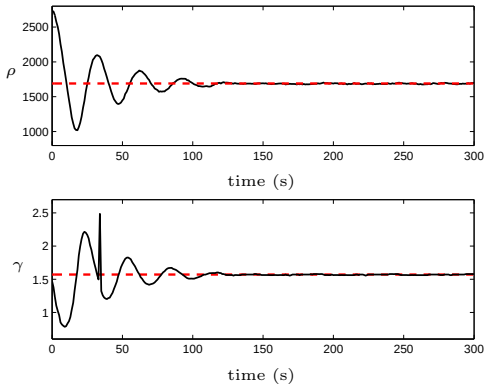

(a) measured ρ and γ

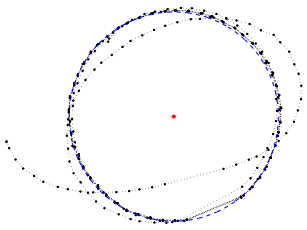

(b) trajectory

Fig. 5. Single-robot experiment: Nomad.

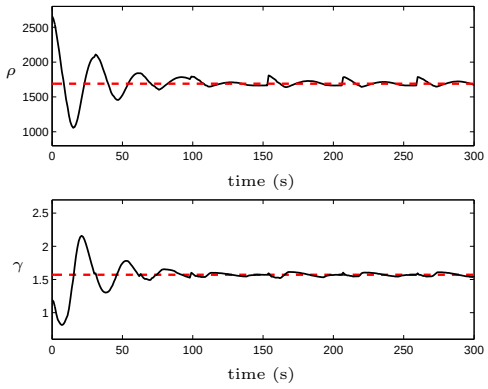

(a) measured ρ and γ

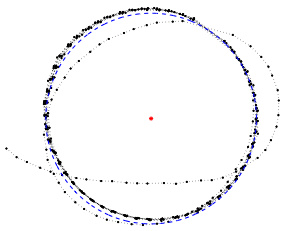

(b) trajectory

Fig. 6. Single-robot experiment: Pioneer.

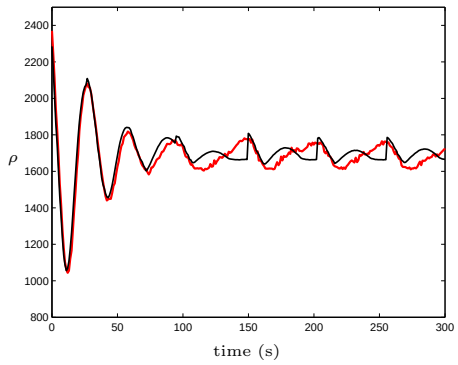

Fig. 7. Odometry effect: $\rho(t)$ estimated by the robot (dark line) and measured by an external sensor (light line).

it. Because of that, when the robot achieves the circular motion, it cannot extract the beacon from the laser readings and odometry-based estimation is required. The odometry drift effect is clearly visible in Figure 7, where the distance $\rho(t)$ estimated by the Pioneer (and used to compute the control input) is compared with the same distance measured by the external laser rangefinder.

Several experimental tests have been performed on the multi-vehicle scenario featuring both robots. We chose $c_v = c_b = 4$, $k_v = 0.2$, so that the sufficient condition (15) is satisfied, and $d_0 = 2\,m$ (recall that (14) is satisfied in this setup). Figures 8 and 9 show the behavior of the multi-vehicle system for different initial conditions. In the figures, ρ_{PN} and γ_{PN} (ρ_{NP} and γ_{NP}) denote respectively the linear and angular distance of the Nomad from the Pioneer (of the Pioneer from the Nomad). At the end of the experiment in Figure 8 the Nomad is behind the Pioneer, while in that of Figure 9 the Pioneer ends up following the Nomad. In both cases one can observe that the inter-vehicle distance $d_0 = 2\,m$ (dashed line in upper Figs. 8(a) and 9(a)) is achieved after a transient and maintained. The same occurs for the equilibrium angular distance between the two robots, given by $\gamma_{ij} = \frac{\pi}{2} - \arccos\left(\frac{d_0}{2\rho_e}\right)$ (dashed line in lower Figs. 8(a) and 9(a)). Figures 8(b)-8(c) and 9(b)-9(c) show the linear and angular distance of each robot from the beacon, confirming that collective circular motion with radius ρ_e is achieved.

A further validation of the results provided by the experimental tests is achieved by comparing the experimental behaviors with the simulation results obtained with the same control law parameters and the same initial conditions. Figures 10 and 11 refer to the same scenario considered respectively in Figures 5 and 6. In both cases the real data (dark line) and simulation data (light line) show almost the same behavior. However, one can notice that the odometry drift is present in Figure 11, and both figures show a sort of

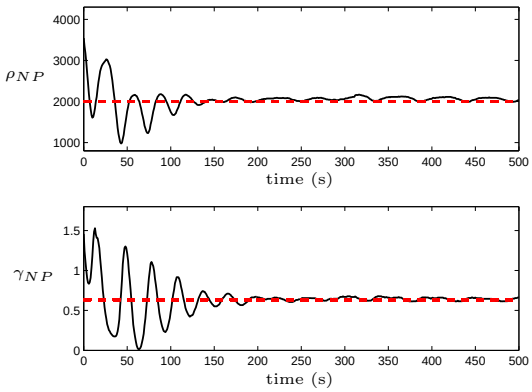

(a) measured ρ_{NP}, γ_{NP}

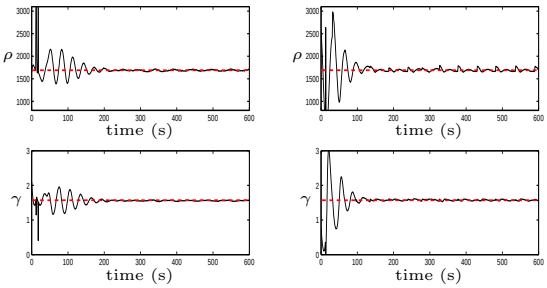

(b) Nomad: ρ,γ (c) Pioneer: ρ,γ

Fig. 8. Multi-vehicle experiment #1.

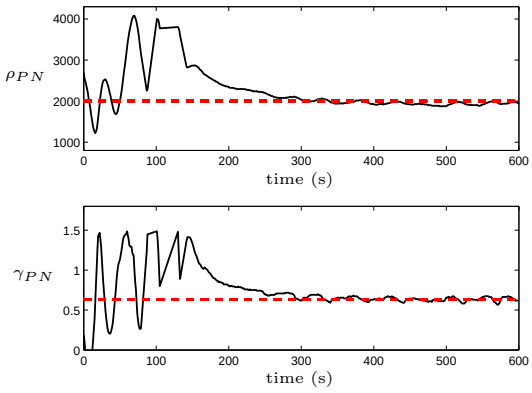

(a) inter vehicles distances: ρ_{PN}, γ_{PN}

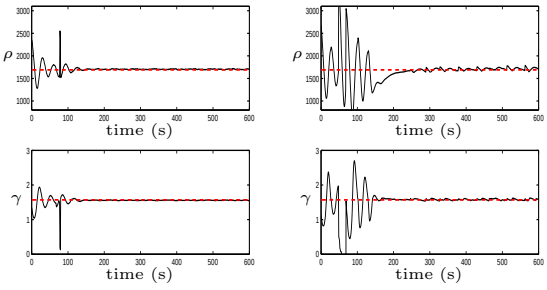

(b) Nomad: ρ,γ (c) Pioneer: ρ,γ

Fig. 9. Multi-vehicle experiment #2.

underdumping effect, mainly due to unmodeled dynamics. Finally, a comparison between experimental and simulation data for the multi-vehicle

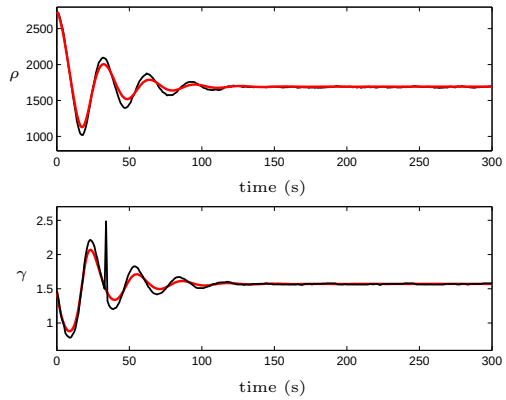

Fig. 10. Comparison between experimental and simulation data: Nomad.

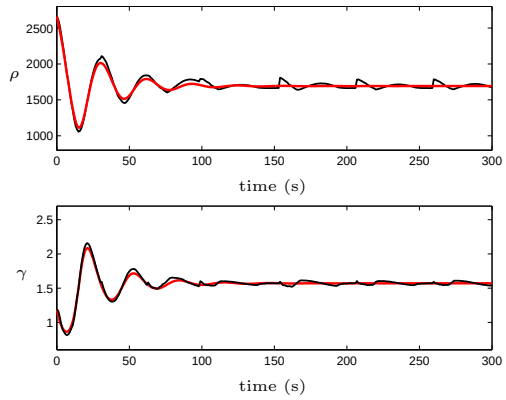

Fig. 11. Comparison between experimental and simulation data: Pioneer.

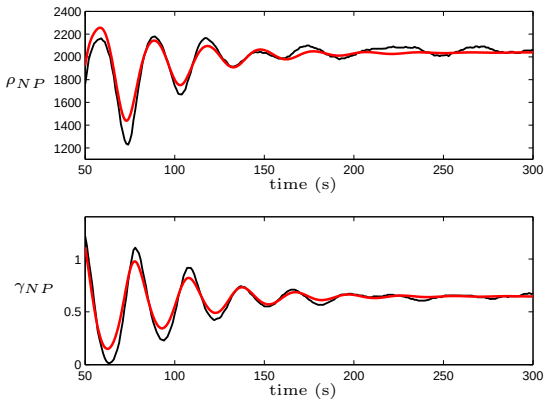

Fig. 12. Comparison between experimental and simulation data: ρ_{NP} and γ_{NP} in multi-vehicle experiment #1.

experiment presented in Figure 8 is reported in Figure 12, where the linear and angular distances ρ_{NP} and γ_{NP} are plotted. Despite the unmodeled dynamics and all the difficulties related with the interaction of different mobile robots moving on an irregular floor, the behavior of the real multi-robot system is quite similar to the one provided by the simulation.

5. CONCLUSIONS

In this paper, experimental validation of a decentralized control law for collective circular motion of multi-vehicle systems has been presented. Tests have been performed on two mobile platforms, moving in a laboratory setup. Experimental results are in good agreement with the simulation runs, in spite of several sources of uncertainty (unmodeled dynamics, measurement noise, processing delays, etc.).

This work represents a first step towards the application of the proposed control scheme on real-world multi-vehicle systems. More extensive validation campaigns are under development, whose aim is to analyze the behavior of larger teams moving in more complex scenarios.

REFERENCES

Arai, T., E. Pagello and L. E. Parker (2002). Special issue on Advances in Multirobot Systems. *IEEE Trans. Rob. Aut.* **18**(5).

Ceccarelli, N., M. Di Marco, A. Garulli and A. Giannitrapani (2005*a*). Collective circular motion of multi-vehicle systems with sensory limitations. In: *Proc. 44th IEEE CDC and ECC 2005*. Seville, Spain. To appear.

Ceccarelli, N., M. Di Marco, A. Garulli and A. Giannitrapani (2005*b*). Stability analysis of collective circular motion for nonholonomic multi-vehicle systems. Tech. Rep. 02/05. DII, Università di Siena. http://control.dii.unisi.it/MobileRoboticsPage/publications/tr02-05.pdf

Jadbabaie, A., J. Lin and A. S. Morse (2003). Coordination of groups of mobile autonomous agents using nearest neighbor rules. *IEEE Trans. Aut. Contr.* **48**(6), 988–1001.

Justh, E. W. and P. S. Krishnaprasad (2004). Equilibria and steering laws for planar formations. *Syst. Contr. Lett.* **52**, 25–38.

Leonard, N. E. and E. Fiorelli (2001). Virtual leaders, artificial potentials and coordinated control of groups. In: *Proc. 40th IEEE CDC*. Orlando. pp. 2968–2973.

Lin, Z., M. E. Broucke and B. A. Francis (2004). Local control strategies for groups of mobile autonomous agents. *IEEE Trans. Aut. Contr.* **49**(4), 622–629.

Marshall, J. A., M. E. Broucke and B. A. Francis (2004). Formations of vehicles in cyclic pursuit. *IEEE Trans. Aut. Contr.* **49**(11), 1963–1974.

Marshall, J. A., T. Fung, M. E. Broucke, G. M. T. D'Eleuterio and B. A. Francis (2005). Experimental validation of multi-vehicle coordination strategies. In: *Proc. 2005 ACC*. pp. 1090–1095.